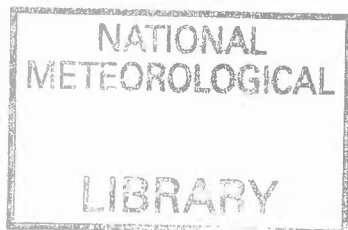


DUPLICATE ALSO



**OCEAN APPLICATIONS TECHNICAL NOTE 5.**

**ON THE LINEAR STABILITY OF LARGE AMPLITUDE BAROTROPIC ROSSBY WAVES IN A PERIODIC ROTATING CARTESIAN CHANNEL.**

by

**M.J.BELL**

**Met Office**

FitzRoy Road, Exeter, Devon. EX1 3PB

**© Crown Copyright 1995**

**This document has not been published. Permission to quote from it must be obtained from the Head of Ocean Applications at the above address.**



## **On the linear stability of large amplitude barotropic Rossby waves in a periodic Cartesian channel**

M. J. Bell, Met. Office, London Rd., Bracknell, RG12 2SZ

September 1995

(Submitted to Quart. J. Roy. Met. Soc.)

### **SUMMARY**

Large amplitude Rossby wave solutions are supported by the quasi-geostrophic equations for a rectangular channel which repeats periodically in the zonal direction with distance  $L_x$  and has rigid side walls distance  $L_y$  apart. This paper concentrates on the stability of waves having the simplest lateral structure with streamfunctions of the form  $\psi_b = \cos 2m\pi x/L_x \sin \pi y/L_y$  ( $m=1,2,\dots$ ). Energy and enstrophy conservation are used together with constraints on the zonally uniform flow to prove that these waves are stable against perturbations which contain only zonal harmonics, both on an  $f$ -plane and a  $\beta$ -plane, when the channel is narrow enough that  $(rm)^2 < 3$ , where  $r = 2 L_y/L_x$  is the aspect ratio of the channel. Numerical results obtained with a spectral model for these waves on an  $f$ -plane suggest that they are stable against normal mode perturbations which contain no zonally uniform modes when  $r^2(m^2-1) < 3$ .

## 1. INTRODUCTION

Monochromatic Rossby waves propagate relative to a uniform zonal flow without changing their shape at a steady rate irrespective of their amplitude. Their properties have been considered in great detail because they are simple enough to be tractable analytically and of value in interpreting large scale waves in the atmosphere and oceans.

For the quasi-geostrophic equations in Cartesian coordinates on an infinite  $\beta$ -plane, barotropic Rossby waves are simple plane waves with streamfunctions of the form:

$$\psi \propto \cos(kx + ly - \omega t + \Phi) \equiv \cos\Theta \quad (1)$$

in which  $k$  and  $l$  are horizontal wavenumbers,  $\omega$  is the angular frequency and  $\Phi$  an arbitrary constant phase angle. In a frame of reference moving with the zonal flow the angular frequency is given by the well-known dispersion relation:

$$\omega = -\beta k / (k^2 + l^2) . \quad (2)$$

The (Jacobian) advection of a second Rossby wave

$$\psi' = \cos(k'x + l'y - \omega't + \Phi') = \cos\Theta' , \quad (3)$$

by  $\psi$  of (1) produces waves with streamfunctions of the form  $\cos(\Theta \pm \Theta')$ . So the linear stability of the wave  $\psi$  to a perturbation *based* on  $\psi'$  involves a "line" of waves (see figure 1) with streamfunctions  $\cos(\Theta' + n\Theta)$  for integer  $n$ . If the horizontal wavenumbers and angular frequency of  $\psi_+ \equiv \cos(\Theta' + \Theta)$  or  $\psi_- \equiv \cos(\Theta' - \Theta)$  also satisfy the Rossby dispersion relation (2), the perturbation is said to be resonant (Pedlosky 1979 section 3.26).

Lorenz (1972) investigated the stability of these waves on an infinite  $\beta$ -plane and found that, for the normal mode disturbances he allowed, a wave of velocity amplitude  $U$  and horizontal wavenumber  $\kappa = (k^2 + l^2)^{1/2}$  was stable when the ratio

$$M = U\kappa^2 / \beta \quad (4)$$

lay below a certain value. Gill (1974) extended Lorenz's work, paying particular attention to the limits of small and large  $M$ . When  $M \ll 1$  only wave perturbations which are almost resonant are unstable. Wave perturbations which are not, tend to drift relative to each other and are hence unable to maintain a constant shape and form normal mode disturbances. At small  $M$ , Gill found coarsely truncated representations of the stability to be reliable. At large  $M$  a wider range of waves is unstable at the coarsest truncation but the truncation is less reliable; it is not valid asymptotically (for  $1/M \rightarrow 0$ ).

The stability of Rossby waves in a finite domain differs from that in an infinite domain in at least two important respects. Firstly the disturbances to the main wave must satisfy the imposed boundary conditions; these greatly restrict the disturbances. Secondly, the main wave whose stability is in question cannot be represented by a single plane wave: it is rather a combination of two plane waves;

$$\begin{aligned}\psi &\propto \cos(2m\pi x/L_x) \sin(\pi y/L_y) \\ &\propto 1/2 \sin(2m\pi x/L_x + \pi y/L_y) - 1/2 \sin(2m\pi x/L_x - \pi y/L_y).\end{aligned}\tag{5}$$

As a result the perturbations are not confined to a line of components as in figure 1 but explore a net of them such as that of figure 2.

Hoskins (1973) and Baines (1976) investigated the stability of barotropic Rossby waves on a sphere:

$$\psi_n^m = P_n^m(\sin\theta) \cos(m\phi - \omega t)\tag{6}$$

where  $P_n^m$  represents an associated Legendre function,  $\theta$  is latitude and  $\phi$  is longitude. Hoskins considered the waves' stability to perturbations including only zonal flows and azimuthal harmonics (i.e. azimuthal wavenumbers 0,  $m$ ,  $2m$ , ..). Baines also considered the stability to waves including other azimuthal wavenumbers (such as sideband instabilities). Baines noted that wave modes  $\psi_1^1$ ,  $\psi_1^0$ ,  $\psi_1^{-1}$  contain the three components of the fluid's angular momentum. Their amplitudes are hence constants of the inviscid motion. The five wave modes with  $n=2$ , which cannot exchange energy amongst themselves, are stable to small amplitude disturbances by Fjortoft's anti-cascade argument, because they cannot transfer energy to modes ( $n=1$ ) with smaller total wavenumbers. Baines found all waves with  $n > 2$  to be unstable when their amplitudes were sufficiently large. Baines and Hoskins found that some very coarse truncations could give moderately accurate representations of the amplitudes of marginal stability and Baines reported that convergence of the solutions was achieved using 30 perturbation modes.

Hoskins (1973 appendix) and Plumb (1977) considered the stability of barotropic Rossby waves of the form (5) in a Cartesian channel of width  $L_y$  and infinite length on a  $\beta$ -plane. Hoskins showed that an instability involving just zonal perturbations and a single harmonic can only occur when the zonal wavelength is less than the width of the channel. The severe truncation used by Hoskins is only valid when  $M$  is small (Pedlosky 1979 section 3.26). Plumb, studying the case  $M \ll 1$ , found (second order) resonant triad instabilities on waves with zonal wavelengths less than 2.937 times the width of the channel. Though waves with longer wavelengths were not unstable to resonant triads Plumb found them to be unstable to (weaker) side-band instabilities.

The stability of Rossby waves of the form (5) in a bounded periodic channel on an  $f$ -plane (or

for that matter a  $\beta$ -plane) appears to have escaped attention. This may be in part because the concept of triad resonances breaks down on an f-plane; all Rossby waves have zero phase velocity and hence all triads are resonant so the resonance criterion does not pick out a small subset of interacting modes. Investigators may also have thought that the problem was of minor importance compared to that for the sphere.

The original motivation for the work which led to the results presented here was to understand the stability of the large amplitude steady waves obtained in thermally forced rotating annulus laboratory experiments (Hide and Mason 1975, Read 1988). These waves can be modelled by free mode combinations of a baroclinic zonal flow and a barotropic wave in a periodic f-plane channel (White 1986). As discussed briefly in section 5, a 3D version of the spectral model described in section 2 was developed to investigate the stability of such combinations.

The paper is structured as follows. Section 2 defines the equations which are taken to govern the flow, derives two constraints on the zonally uniform flow, outlines the spectral numerical model used to obtain the numerical results, describes the waves whose stability is examined and illustrates the truncations used in the numerical calculations. Section 3 establishes a stability condition for perturbations which contain only zonal harmonics (including zonally uniform components). Numerical results for the stability of other disturbances on an f-plane are presented in section 4. Section 5 summarises the results and discusses their relevance to the rotating annulus experiments and to a range of problems for which the f-plane channel represents a limiting case.

## 2. PROBLEM POSED AND METHODS USED

### (a) Equations governing the flow

The quasi-geostrophic equations for a barotropic fluid are taken to govern the motion. In Cartesian coordinates  $(x, y, z)$  with the horizontal velocity  $\mathbf{u} = (u, v)$ ,  $p$  denoting pressure,  $\rho^*$  a constant density and the subscript  $g$  the geostrophic motion, these are:

$$\begin{aligned}\rho^* (\partial u_g / \partial t + (\mathbf{u}_g \cdot \nabla) u_g - f v) + \partial p / \partial x &= 0 \\ \rho^* (\partial v_g / \partial t + (\mathbf{u}_g \cdot \nabla) v_g + f u) + \partial p / \partial y &= 0 \\ \partial u_g / \partial x + \partial v_g / \partial y &= 0.\end{aligned}\tag{7}$$

In section 3 the Coriolis parameter  $f$  is allowed to depend on the ordinate perpendicular to the side-wall but in section 4 it is limited to a constant (the  $f$ -plane).

The geostrophic velocities can be written in terms of a streamfunction:

$$u_g = -\partial \psi / \partial y ; \quad v_g = \partial \psi / \partial x\tag{8}$$

and the evolution of the streamfunction is determined by the boundary conditions and the barotropic vorticity equation:

$$\partial \zeta / \partial t + J(\psi, f + \zeta) = 0\tag{9}$$

in which the Jacobian  $J(a, b) \equiv \partial a / \partial x \partial b / \partial y - \partial b / \partial x \partial a / \partial y$  and the relative vorticity

$$\zeta = L(\psi) ; \quad L \equiv \nabla_h^2 = \partial^2 / \partial x^2 + \partial^2 / \partial y^2.\tag{10}$$

The Cartesian channel is periodic in  $x$  with repeat distance  $L_x$  and has rigid side-boundaries at  $y = 0, L_y$  where

$$\partial \psi / \partial x = 0.\tag{11}$$

### (b) Derivation of boundary conditions on the zonal mean flow

Integration of the  $x$ -component of the momentum equation over the channel provides a constraint on the zonal mean streamfunction at the sidewalls:

$$\iint \rho^* (\partial u_g / \partial t + (\mathbf{u}_g \cdot \nabla) u_g - f v) + \partial p / \partial x \, dx \, dy = 0.\tag{12}$$

Integration of the pressure gradient in  $x$  and use of the periodic boundary conditions shows that term to provide no contribution. Using the continuity equation and the condition of no normal flow at the sidewalls one can show that

$$\int v \, dx \equiv \bar{v} = 0, \quad (13)$$

the overbar representing the zonal mean. So the integral of the Coriolis term is zero for any  $f(y)$ . The integral of the advection term is also zero as may be shown by integrating by parts and using the continuity equation. Thus

$$d/dt \int u_g \, dx \, dy = 0 \Rightarrow d/dt \{ \bar{\Psi}(L_y) - \bar{\Psi}(0) \} = 0 \text{ for any } f(y). \quad (14)$$

For the flows investigated in this paper the zonal flow is initially uniform (i.e. independent of  $y$ ). The frame of reference may be chosen so that the wave whose stability is being investigated is stationary. In this frame of reference the initial zonal velocity  $\bar{u}$  is equal and opposite to the Rossby wave's phase speed. Let the zonal flow associated with the perturbation to the wave flow be  $\chi$ :

$$\bar{\Psi} = y\bar{u} + \chi. \quad (15)$$

From (14)  $\chi$  must take the same value at the two sidewalls. An arbitrary constant which is a function of time only,  $d(t)$ , may be added to the streamfunction without changing the flow. This constant may be chosen so that the streamfunction at  $y=0$  is zero at all times and thus so that

$$\chi = 0 \text{ at } y=0 \text{ and } y=L_y. \quad (16)$$

Conditions on the lateral gradient of the zonal mean streamfunction at the sidewalls can be obtained from the zonal mean of the barotropic vorticity equation:

$$\partial/\partial t (\partial^2 \bar{\Psi} / \partial y^2) + \partial/\partial y (\bar{v}_g \nabla^2 \bar{\Psi}') = 0. \quad (17)$$

the primes denoting the eddy part of the flow (that is the quantity minus its zonal mean). This equation can be integrated with respect to  $y$  twice:

$$\begin{aligned} \partial/\partial t (\partial \bar{\Psi} / \partial y) + \bar{v}_g \nabla^2 \bar{\Psi}' &= c(t) \\ \partial \bar{\Psi} / \partial t - \bar{v}_g u_g' &= y c(t) + d(t). \end{aligned} \quad (18)$$

As  $v_g' = 0$  at the sidewalls (15) and (16) imply that  $c(t) = d(t) = 0$  in (18) and hence that

$$\partial\chi/\partial y = 0 \text{ at } y=0 \text{ and } y=L_y. \quad (19)$$

Hence the zonal flow is constrained by both boundary conditions (15) and (19) each of which is by itself energy conserving and consistent with the zonal momentum equation (Pedlosky 1979 section 7.2).

### (c) Description of the numerical spectral model

The spectral model is an implementation of that described in Bell & White (1988) which builds on the ideas of Charney (1971) for 3D internal baroclinic jets. For the 2D problem which is the focus of this paper the main properties were established by Lorenz (1960). The model uses as its basis functions the eigenfunctions of the operator  $L$ , defined in (10), which satisfy the boundary conditions (11) and (16) or (19):

$$L\psi_i = -\lambda_i^2 \psi_i \quad ; \quad \psi = y\bar{u} + \sum_{i=1}^N a_i \psi_i. \quad (20)$$

The eigenvalues  $\lambda_i$  will be described as the total or horizontal wavenumbers for the corresponding eigenfunctions which will usually be referred to as components. The Sturm Liouville form of (10) and its boundary conditions ensures that these basis functions are orthogonal:

$$\langle \psi_i, \psi_j \rangle = \int \int \psi_i \psi_j dx dy = \langle \psi_i, \psi_i \rangle \delta_{ij}. \quad (21)$$

Multiplication of (9) by  $\psi_i$  and integration over the domain yields an equation for the rate of change of  $a_i$ :

$$\begin{aligned} \lambda_i^2 da_i/dt \langle \psi_i, \psi_i \rangle = & - \sum_{j=1}^N \sum_{k=1}^N \lambda_k^2 a_j a_k \langle \psi_i, J(\psi_j, \psi_k) \rangle \\ & + b_i (\beta_i - \lambda_i^2 \bar{u}) \langle \psi_i, \partial \phi / \partial x \rangle \end{aligned} \quad (22)$$

In (22),  $\phi_i$  represents the component with the same lateral structure and azimuthal wavenumber as  $\psi_i$  which is  $\pi/2$  radians out of phase with  $\psi_i$ , and  $b_i$  its amplitude.  $\psi_i$  and  $\phi_i$  will be referred to as a pair of components.

By integration by parts and use of the boundary conditions the overlap integral  $\langle \psi_i, J(\psi_j, \psi_k) \rangle$

can be shown to have the associative and commutative properties of a triple product:

$$\langle \psi_i J(\psi_j, \psi_k) \rangle = \langle \psi_k J(\psi_i, \psi_j) \rangle = -\langle \psi_j J(\psi_k, \psi_i) \rangle . \quad (23)$$

The analogues of energy and enstrophy in this system are:

$$E_A = 1/2 \sum_{i=1}^N \lambda_i^2 a_i^2 \langle \psi_i \psi_i \rangle ; \quad F_A = 1/2 \sum_{i=1}^N \lambda_i^4 a_i^2 \langle \psi_i \psi_i \rangle \quad (24)$$

Using (23) in (22) Lorenz (1960) showed that these analogues are conserved by interactions between any three components when  $\beta = 0$ . When  $\beta \neq 0$ , interactions between any **three pairs** of components conserve  $E_A$  and  $F_A$ . Energy and enstrophy are hence conserved in all truncations of the spectral model and the model has the anti-cascade property.

The numerical implementation of the spectral model, for a given truncation (see below), determines which overlap integrals are non-zero, calculates their values and those of  $\langle \psi_i \psi_i \rangle$ ,  $\langle \psi_i \phi_i \rangle$  and  $\lambda_i$ . The formulation used for the results presented in sections 3 & 4 seeks the normal modes of (22) by setting  $da_i/dt = \gamma a_i$  and solving the resulting matrix equation for the eigenvalue  $\gamma$ . The growth rates presented have been normalised by multiplying by  $L_y/U$  where  $U$  is the maximum zonal velocity of the basic wave-like flow and so are non-dimensional.

#### (d) Description of waves examined and truncations used

The waves whose stability is to be considered have streamfunctions,  $\psi_0$ , of the form:

$$\psi_0 = \bar{u}y + \psi_b \text{ with } \psi_b = UL_y/\pi \cos 2m\pi x/L_x \sin \pi y/L_y . \quad (25)$$

$\psi_b$  has total wavenumber

$$\lambda_b^2 = (r^2 m^2 + 1) \pi^2 / L_y^2 \text{ where } r \equiv 2L_y/L_x . \quad (26)$$

For brevity "the streamfunction of a component" will be referred to simply as "the component" and, to make the notation easier to read, components will be written using the non-dimensional coordinates

$$x' \equiv \frac{2\pi x}{L_x} ; \quad y' \equiv \frac{\pi y}{L_y} . \quad (27)$$

The interaction of a small amplitude component,  $\cos nx' \sin y'$  with  $\psi$  produces small amplitude components  $\sin(m \pm n)x' \sin y'$ . The interaction of these with  $\psi$  produces further components. The net of components produced on an f-plane is illustrated by figure 2. We shall say that a perturbation is based on the component contained in it which has the smallest zonal wavenumber and  $\sin y'$  lateral structure. The net illustrated in figure 2 extends up to arbitrarily large wavenumbers and must be truncated for the purposes of numerical calculations. The "square" truncation which has been used includes at level P all components with lateral wavenumber  $\leq P$  and azimuthal wavenumber  $< mP$ . The truncation at level P includes  $P^2$  perturbation components. On a  $\beta$ -plane the paired component of each of these components is also produced and the corresponding truncations would include  $2P^2$  components. It is not immediately clear that perturbations to  $\psi$  based on  $\sin mx' \sin y'$  will yield the same eigenvalues as those based on  $\cos mx' \sin y'$ . Comparison of the overlap sums for the two cases, however, reveals a symmetry between them and they do have the same eigenvalues.

Figure 3 illustrates the components induced on an f-plane by a perturbation based on the zonally independent component  $\sin y'$  which satisfies boundary condition (16). Again on a  $\beta$ -plane the paired component of each component is also produced.

### 3. Stability of disturbances based on zonally uniform components

The wave (25) can be shown to be stable to all disturbances including only harmonics of its zonal wavenumber by a version of Fjortoft's anti-cascade argument. The wave-like components of the harmonics are simple sinusoidal functions so their energy,  $E_w$ , and enstrophy,  $F_w$ , are simply sums of the squares of their amplitudes,  $a_w$ , multiplied by powers of their total wavenumbers:

$$E_w = \frac{1}{2} \sum_w \lambda_w^2 a_w^2; F_w = \frac{1}{2} \sum_w \lambda_w^4 a_w^2. \quad (28)$$

In the frame of reference in which  $\bar{u} = 0$  the energy,  $\xi$ , and enstrophy,  $F$ , of the zonal flow depend only on  $\partial\chi/\partial y$  and  $\partial^2\chi/\partial y^2$ :

$$\xi(\chi) = \iint (\partial\chi/\partial y)^2 dx dy; F(\chi) = \iint (\partial^2\chi/\partial y^2)^2 dx dy. \quad (29)$$

Let  $\{\rho_i\}$  be a complete set of functions of functions which satisfy the boundary conditions for  $\chi$ . Then one can set

$$\chi = \sum_i a_i \rho_i. \quad (30)$$

If the functions  $\partial\rho_i/\partial y$  are mutually orthonormal and the functions  $\partial^2\rho_i/\partial y^2$  are also mutually orthonormal then the energy and enstrophy of the zonal flow will be of the form:

$$\xi = \frac{1}{2} \sum_i \lambda_i^2 a_i^2; F = \frac{1}{2} \sum_i \lambda_i^4 a_i^2 \quad (31)$$

and Fjortoft's argument can be applied.

Familiarity with Sturm-Liouville theory suggests that the functions for which  $F/\xi$  is stationary to all variations which satisfy the boundary conditions might be such a set of functions. That this is indeed the case can be verified by considering the variational problem:

$$\delta \{F(\rho) - \lambda^2 \xi(\rho)\} = 0; \rho = \partial\rho/\partial y = 0 \text{ at } y=0, L_y. \quad (32)$$

The eigenvalue problem resulting from (32) is

$$\partial^4 \rho / \partial y^4 + \lambda^2 \partial^2 \rho / \partial y^2 = 0 \quad (33)$$

(with the same boundary conditions as in (32)). That the first and second derivatives of these functions are mutually orthogonal as required can be established in the same manner as for Sturm-Liouville problems (as in Kreyszig 1979 p191). The general solution to (33) is

$$\rho = Ay + B + C\cos\lambda y + D\sin\lambda y . \quad (34)$$

Applying the boundary conditions at  $y=0$  one finds that  $B = -C$  and  $A = -\lambda D$ . Applying them then at  $y=L_y$  one obtains:

$$C(\cos\lambda' - 1) - D(\lambda' - \sin\lambda') = 0 ; \lambda' D(\cos\lambda' - 1) - \lambda' C\sin\lambda' = 0 . \quad (35)$$

where  $\lambda' = \lambda L_y$ . Eliminating  $D$  one finds that for non-zero solutions

$$\lambda' \sin\lambda' = 2(1 - \cos\lambda') \Rightarrow \sin\lambda'(\tan\lambda'/2 - \lambda'/2) = 0 . \quad (36)$$

The solutions for  $\sin\lambda' = 0$  are:

$$\rho_n = 1 - \cos 2n\pi y/L_y ; \lambda_n = 2n\pi/L_y . \quad (37)$$

The first solution for  $\tan\lambda'/2 = \lambda'/2$  has  $\lambda = 1.4303 (2\pi/L_y)$ .

The ratio of the enstrophy divided by the energy ( $F_w/E_w$ ) for any wave-like zonal harmonic is greater than that for the wave (25) whose stability is in question. All the zonally uniform modes just derived also have a larger ratio when

$$\lambda_b^2 < (2n\pi/L_y)^2 \Rightarrow (rm)^2 < 3 . \quad (38)$$

Since energy and enstrophy are conserved it is then clear that there can be no perturbations which grow without changing their shape when  $(rm)^2 < 3$ .

Bounds on the growth in the energy and enstrophy of zonally harmonic perturbations of arbitrarily evolving shape and amplitude can be derived by considering the changes in the energy,  $\Delta E$ , and enstrophy,  $\Delta F$ , of the main wave; the changes in the energy and enstrophy of the perturbation are  $-\Delta E$  and  $-\lambda_b^2 \Delta E$ . Let  $E_i$  and  $F_i$  be the initial energy and enstrophy of a perturbation and let the ratio of the final enstrophy,  $F_F$ , to the final energy,  $E_F$ , of the perturbation be  $\lambda^2$ :

$$\lambda_b^2 \Delta E = \Delta F ; \lambda^2 E_F \equiv F_F , \quad (39)$$

By energy and enstrophy conservation

$$E_F = E_I - \Delta E ; \lambda^2 E_F = F_I - \lambda_b^2 \Delta E . \quad (40)$$

So the change in energy of the perturbation is

$$-\Delta E = \frac{F_I - \lambda^2 E_I}{(\lambda^2 - \lambda_b^2)} < \frac{F_I}{(\lambda^2 - \lambda_b^2)} \text{ when } \lambda^2 > \lambda_b^2 . \quad (41)$$

The last inequality holds when  $(rm)^2 < 3$ .

Although this argument shows that the wave is stable to non-linear harmonic perturbations in a strong sense it does not show that the phase of the wave progresses completely steadily. The main wave has tacitly been taken to include both the  $\cos 2m\pi x/L_x \sin \pi y/L_y$  and  $\sin 2m\pi x/L_x \sin \pi y/L_y$  components of the flow. Variations in the phase velocity of the main wave have not been ruled out. Benjamin's (1972) analysis of the stability of solitary waves similarly distinguished changes in the shape of the solitary wave from changes in their phase speed in proving their stability.

The above arguments also do not establish that  $(rm)^2 = 3$  is a significant stability transition point. To pursue this point it is useful to consider the equation for the linear stability of the wave in the frame of reference in which the main wave is stationary. In this frame  $\beta = \lambda_b^2 \bar{u}$ . Letting  $\psi = \bar{u}y + \psi_b + \psi_p$  and ignoring terms involving the square of the perturbation streamfunction  $\psi_p$ , the vorticity equation (9) can be manipulated into the form

$$\partial \zeta / \partial t + J(\bar{u}y + \psi_b, \zeta + \lambda_b^2 \psi) = 0 \quad (42)$$

$\rho_1$  as given by (37) is a free mode solution of (42) when  $(rm)^2 = 3$  (and hence  $\lambda_1 = \lambda_b$ ). But  $\rho_1$  has (its maximum) vorticity at the sidewalls. For a disturbance to grow it must re-distribute the absolute vorticity of the basic flow so as to increase its own vorticity. Now the relative vorticity of the main wave and the lateral velocity of the wave and perturbations are zero at the sides and grow no faster than linearly with distance into the interior. The rate at which vorticity will be advected towards the sidewalls will be no faster than proportional to the distance from them. The time taken for a given vorticity to reach distance  $\delta y$  from the sides will be proportional to  $-\ln \delta y$ . So normal mode disturbances cannot grow from the solution at  $(rm)^2 = 3$ .

The solutions with  $\tan\lambda/2 = \lambda/2$  have

$$\partial^2 \rho / \partial y^2 + \lambda^2 \rho = \lambda^2 (Ay + B) \Rightarrow J(\psi_b, \partial^2 \rho / \partial y^2 + \lambda^2 \rho) = \lambda^2 A \partial \psi / \partial x \quad (43)$$

Since  $B$  is non-zero these solutions also have non-zero vorticity at  $y=0$ . When their enstrophy to energy ratio matches that of the basic wave (25) they provide free mode solutions in which the drift rate of the basic wave differs from  $\bar{u}$ .

A simple form for  $\chi$  which has zero vorticity at the sides and satisfies the boundary condition is

$$\chi \propto (3 \sin y' - \sin 3y') \quad (44)$$

which has the same enstrophy to energy ratio as the main wave when  $rm = 2$ . Hoskins (1973 appendix) derived this values for the stability transition by calculating the rate of transfer of energy from the first harmonic of the main wave into the two zonal components included in (44) and assuming that other interactions could be neglected. This streamfunction is not a neutral solution of (42) for  $rm = 2$ , so it too cannot mark a normal mode stability transition.

Numerical results provide some indication of where the stability transition for normal modes might be. Tables 1 and 2 present results from the spectral model described in section 3c for the stability of  $\psi_b$  on an  $f$ -plane using a sine function expansion in  $y'$  for  $\chi$  and the truncations illustrated in Figure 3. Table 1 shows that for values of  $rm = 2/3$ , for which the flow is definitely stable, even truncations of the spectral model support unstable modes. This result can be interpreted in terms of the truncation error of (17) and (18). In the odd truncations the components of  $J(\psi, \zeta)$  which are truncated do not include zonally uniform modes. So (19) holds for the odd truncations. For the even truncations this is not the case; for  $P=2$ , for example, modes included in the truncation for  $\psi$  and  $\zeta$  will generate amplitude in the component  $\sin 3y'$  of  $J(\psi, \zeta)$  which is truncated. Table 2 indicates the location of the transition to normal modes for odd truncations  $P=5, 7$  and  $13$ . It seems likely that on an  $f$ -plane the wave becomes unstable to normal modes for  $rm > 2.2$ .

#### 4. Numerical results on the stability of perturbations based on wave components on an f-plane

Table 3 displays the eigenvalues of the most unstable normal mode perturbations to (25) with  $m=2$  based on  $\cos x' \sin y'$  for two values of the aspect ratio,  $r$ :  $r=1/3$  and  $r=1$ . At both these aspect ratios all truncations with odd values of  $P$  have no unstable components and the instability found with even truncations decreases rapidly in strength as  $P$  increases. These results suggest that the main wave is stable to this wave perturbation at both aspect ratios. The significant difference between coarse even and odd truncations is a characteristic of all results presented here.

Stability transitions, according to truncations with  $P=13$ , for  $\psi$  given by (25) with  $m=2, 3$  and  $4$  and perturbations based on  $\cos nx' \sin y'$  are tabulated in table 4. The  $m=2$  wave is evidently marginally stable at  $r = 1.0$ . At this aspect ratio,  $\sin x' \sin 2y'$ , a prominent member in the net of perturbation components, has the same total wavenumber as the main wave. Some of the interactions with other components and the corresponding terms in the stability matrix will change sign at this critical aspect ratio. At higher aspect ratios than the critical, two components will have smaller total wavenumber than the main wave so energy cascades will have more freedom.

Table 4 also shows that the wave (25) with  $m=3$  has a smaller critical aspect ratio for perturbations based on  $\cos 2x' \sin y'$  than  $\cos x' \sin y'$ . The net of components based on the former includes  $\sin x' \sin 2y'$ , which has a lower total wavenumber than its counterpart  $\sin 2x' \sin 2y'$  in the  $\cos x' \sin y'$  net. The component  $\sin x' \sin 2y'$  has the same total wavenumber as the main wave when  $(9-1)r^2 = 3$ ; i.e.  $r = 0.6124$ , whilst  $\psi = \sin 2x' \sin 2y'$  has the same total wavenumber as the main wave when  $(9-4)r^2 = 3$ ; i.e.  $r = 0.7746$ . Inspection of table 4 shows that the transitions for  $P = 13$  must be very close to these values if not identical with them. A similar argument for  $m=4$  and  $n=3$  locates the transition at  $r = 0.4472$  for which  $\sin x' \sin 2y'$  has the same wavenumber as  $\cos 4x' \sin y'$  (i.e.  $(16-1)r^2 = 3$ ) in agreement with table 4. But for  $m=4$  and  $n=1$  it locates the transition at  $r = 0.6547$  (when  $\sin 3x' \sin 2y'$  has the same wavenumber as  $\cos 4x' \sin y'$ , i.e.  $(16-9)r^2 = 3$ ) which is a significantly larger value than that found numerically and recorded in table 4.

The above result for  $m=4$  and  $n=1$  suggests that two wave components with smaller total wavenumber than the main wave are not always needed for a net of components to contain instabilities but is consistent with the

**Hypothesis:** that the barotropic wave (25) is stable to normal mode perturbations based on wave components when  $r^2(m^2-1) < 3$ .

The results in table 5 show that the transition for the  $m=2$  flow is located exactly at  $r=1.0$  by both  $P=3$  and  $P=5$  truncations, but that the growth rate in the unstable region near the transition is over-estimated by these coarse truncations. The transition to healthy instability is remarkably

sharp even for the  $P=13$  truncation. Indeed the eigenvalue appears to depend on the square root of the supercriticality of the aspect ratio (i.e. on  $(r-1)^{1/2}$ ). Table 5 also reveals that the instability does not increase monotonically with  $r$ ; the  $P=13$  truncation shows a return to stability for  $1.2 \leq r \leq 1.3$ . Similar returns to stability for the  $P=3$  and  $P=5$  truncations occur for  $1.4 \leq r \leq 1.5$  and for the  $P=12$  truncation for  $1.3 \leq r \leq 1.4$ . Clearly the aspect ratio at which stability might return in the continuous (untruncated) problem cannot be reliably inferred from table 5.

"Odd" truncations with  $P=3$  and  $P=5$  have also been found to locate the stability transition in agreement with the hypothesis for perturbations based on  $\cos 2x' \sin y'$  when  $m=3$ . An indication of the convergence of the even truncations of this perturbation is presented in table 6. As in table 3,  $r$  is well below the critical value ( $r=0.6124$ ) in the first column and close to it in the second. The convergence of the first column towards zero is rapid but that of the second is at best very slow and much worse than that of table 3.

### 5. Concluding discussion

The two main results of this paper concern the stability of barotropic waves in a periodic Cartesian channel with streamfunctions of the form (25). They may be summarised as :

1. waves of this form, regardless of their amplitude on both an f-plane and a  $\beta$ -plane are stable against barotropic quasi-geostrophic disturbances which contain only zonal harmonics (of the wave (5)) when  $(rm)^2 < 3$ . This is proved in section 3 using an anti-cascade argument and constraints on the zonally uniform flow components.
2. numerical results on the stability of such waves on an f-plane against normal mode disturbances containing no zonally uniform components suggest the hypothesis that the waves are stable against such normal modes when  $r^2(m^2-1) < 3$ .

Further work, beyond the scope of this paper, would be useful to confirm or reject this hypothesis and to explore the senses in which the waves are stable if it is true. The most enticing approach is to seek additional conservation relations or constraints which can account for the numerical results when used with the energy and enstrophy constraints in the spirit of section 3. Further investigation of the structure of the apparently spurious unstable modes in the spectral model with even truncations might be illuminating. The truncation with  $P=2$  can be treated analytically and could hence be particularly informative.

The spectral model outlined in section 2(c) can be applied to three-dimensional flows with internal jet boundary conditions

$$\partial\psi/\partial z = 0 \text{ at upper and lower boundaries at } z=0, H \quad (45)$$

which appear to be relevant to the differentially heated rotating annulus experiments (White 1986). I discovered the results described in section 4 whilst attempting to study the stability of a free mode of the form suggested by White (1986):

$$\frac{\psi}{UL_y} = \frac{a_0}{\pi} \cos \pi z/H \sinh \pi(y/L_y - 1/2) + \frac{1-a_0}{\pi} \cos 4\pi x/L_x \sin \pi y/L_y. \quad (46)$$

As described in Bell (1989), numerical results suggest that for  $r=1/3$  the above wave is stable when  $a_0 < 0.25$  and is unstable when the zonal flow is stronger. So according to these results, on this zonal flow the **wave is only stable when it is of relatively large amplitude** relative to the zonal flow.

The stability criterion  $rm < 3^{1/2} \approx 1.7$  agrees quite well with the maximum wavenumber of the

waves found in the annulus experiments. According to table 5 of Hide & Mason (1975) the maximum wavenumber corresponds to values of  $rm$  between 1.3 and 1.4. Further study of the stability of the waves of forms like (46) might well provide useful insight into the steady waves which can be obtained into the annulus experiments. Constraints corresponding to (14) and (18) can be derived for flows in cylindrical annuli by using cylindrical coordinates. For example angular momentum conservation

$$d/dt \int s u_g s ds d\phi = 0 \quad \text{for any } f(s). \quad (47)$$

corresponds to (14). (In (47)  $s$  denotes radial distance from the axis,  $\phi$  is the azimuthal angle about the axis,  $u$  is the azimuthal flow and  $f$  is the Coriolis parameter).

The stability of waves on an  $f$ -plane in a periodic channel stands as a limiting case of many problems; for example:

- (a) large amplitude waves in a  $\beta$ -plane channel
- (b) waves in a cylindrical annulus
- (c) free modes consisting of a barotropic wave on a baroclinic zonal flow

For this reason the problem is of quite wide interest but is also likely to mark a stability boundary for only some of these problems (c.f. Eady's stability problem; McIntyre 1970). The elucidation of how these problems relate to the one considered here would greatly extend the value of this paper.

### Acknowledgement

I particularly wish to thank Dr. A. A. White who initiated and supervised this work and suggested the argument leading from (16) to (19).

### References

- Baines, P. G., 1976 The stability of planetary waves on a sphere. *J. Fluid Mech.*, **73**, 193-213.
- Bell, M. J., 1989 Theoretical Investigations prompted by experiments with baroclinic fluids. Ph. D. Thesis, Imperial College, London.
- Bell, M. J., and A. A. White, 1988 The stability of internal baroclinic jets: some analytical results. *J. Atmos. Sci.*, **45**, 2571-2590.
- Benjamin, T. B., 1972 The stability of solitary waves. *Proc. Roy. Soc. Lond. A*, **328**, 153-183.
- Charney, J. G., 1971 Geostrophic turbulence. *J. Atmos. Sci.*, **28**, 1087-1095.
- Gill, A. E., 1974 The stability of planetary waves on an infinite beta-plane. *Geophys. Fluid Dyn.*, **6**, 29-47.
- Hide, R., and P. J. Mason, 1975 Sloping convection in a rotating fluid: a review. *Advances in Phys.*, **24**, 47-100.
- Hoskins, B. J., 1973 Stability of the Rossby-Haurwitz wave. *Quart. J. Roy. Meteor. Soc.*, **99**, 723-745.
- Kreyszig, E. 1979 *Advanced Engineering Mathematics*. New York, Wiley, 939 pp.
- Lorenz, E. N., 1960 Maximum simplification of the dynamic equations. *Tellus*, **12**, 243-254.
- Lorenz, E. N., 1972 Barotropic instability of Rossby wave motion. *J. Atmos. Sci.*, **29**, 258-264.
- McIntyre, M. E., 1970 On the non-separable baroclinic parallel-flow instability problem. *J. Fluid Mech.*, **40**, 273-306.
- Pedlosky, J., 1979 *Geophysical Fluid Dynamics*. Springer Verlag, New York, 624 pp.
- Plumb, R. A., 1977 The stability of small amplitude Rossby waves in a channel. *J. Fluid Mech.*, **80**, 705-720.
- Read, P. L., 1988 The dynamics of rotating fluids: the 'philosophy' of laboratory experiments and studies of the atmospheric general circulation. *Met. Mag.*, **117**, 35-53.
- White, A. A., 1986 Finite amplitude, steady Rossby waves and mean flows: analytical illustrations of the Charney-Drazin non-acceleration theorem. *Quart. J. Roy. Meteor. Soc.*, **112**, 749-773.

### Table Captions

Table 1: Truncation dependence of the non-dimensional growth rate of the most unstable normal mode perturbation based on  $\chi = \sin y'$  to the wave of the form (25) for  $rm=2/3$  and  $rm=2$  on an f-plane. "S" indicates that all normal modes are (neutrally) stable.

Table 2: Bounds on the value of  $rm$  of marginal stability for perturbations based on  $\chi = \sin y'$  to the wave of the form (25) on an f-plane as a function of truncation level  $P$ . The lower bound is written in the table; the upper bound is the lower bound plus 0.01.

Table 3: Truncation dependence of the non-dimensional growth rate of the most unstable normal mode perturbation based on  $\cos x' \sin y'$  to the wave of the form (25) with  $m=2$  on an f-plane for channel aspect ratios  $r=1/3$  and  $r=1$ . "S" indicates that all normal modes are (neutrally) stable.

Table 4: Bounds on the channel aspect ratio ( $r$ ) of marginal stability for wave perturbations based on  $\cos mx' \sin y'$  to the wave of the form (25) on an f-plane for values of  $m$  between 2 and 4. The truncation level is  $P=13$  in all cases and  $\gamma_r$  is the perturbation's non-dimensional growth rate.

Table 5: Dependence on the truncation level  $P$  and the channel aspect ratio  $r$  of the growth rate,  $\gamma_r$ , of the most unstable normal mode perturbation based on  $\cos x' \sin y'$  to a wave of the form (25) with  $m=2$  on an f-plane. "S" indicates that all normal modes are (neutrally) stable.

Table 6: Truncation dependence of the non-dimensional growth rate of the most unstable normal mode perturbation based on  $\cos 2 x' \sin y'$  to the wave of the form (25) with  $m=3$  for an f-plane and channel aspect ratios  $r=0.3$  and  $r=0.6$ .

**Figure captions**

Figure 1: The "line" of perturbation components involved in the linear stability of a plane wave with streamfunction  $\psi$  given by (1). The components are represented by points on the horizontal wavenumber plane  $(k,l)$ . The main wave has wavenumber  $\mathbf{k}$ . Its linear stability to a perturbation  $\psi'$  given by (3) with wavenumber  $\mathbf{k}'$  is at issue. The advection of the vorticity of  $\psi$  by  $\psi'$  only produces components  $\psi_+$  and  $\psi_-$ . The interaction of these and subsequent components with  $\psi$  produces only the components lying on the line of wavenumbers illustrated.

Figure 2: The components included in truncations  $P=1$  to  $P=4$  for a perturbation to the wave of the form (5) based on  $\cos nx' \sin y'$ .  $x' \equiv 2\pi x/L_x$  and  $y' \equiv 2\pi y/L_y$  are non-dimensional co-ordinates.

Figure 3: The first few components generated by a perturbation to the wave of the form (25) based on  $\sin y'$ .

**Table 1**

Truncation level (P)	Growth rate	
	rm = 2/3	rm = 2
3	S	S
4	$5.16 \cdot 10^{-2}$	1.56
5	S	S
6	$5.04 \cdot 10^{-3}$	1.05
9	S	S
10	$1.82 \cdot 10^{-4}$	0.532
15	S	S
16	$5.36 \cdot 10^{-7}$	0.224

**Table 2**

Truncation (P)	lower bound on rm
5	2.34
7	2.32
13	2.28

**Table 3**

r=1/3		r=1	
Truncation level (P)	Growth rate	Truncation level (P)	Growth rate
2	$1.51 \cdot 10^{-1}$	2	$7.55 \cdot 10^{-1}$
3	S	3	S
4	$1.85 \cdot 10^{-2}$	4	$9.80 \cdot 10^{-2}$
5	S	5	S
8	$6.39 \cdot 10^{-4}$	8	$4.47 \cdot 10^{-3}$
9	S	9	S
		12	$1.75 \cdot 10^{-4}$
		13	S

**Table 4**

Azimuthal wavenumbers				
m	n	r	$\gamma_r$	$\gamma_i$
2	1	1.000	0.0	0.0
		1.005	0.116	0.0
3	1	0.77	0.0	0.077
		0.78	0.065	0.0
3	2	0.610	0.0	0.087
		0.615	0.091	0.0
4	1	0.585	0.0	0.003
		0.59	0.195	0.0
4	3	0.44	0.0	0.153
		0.45	0.097	0.0

**Table 5**

r	P=3	P=5	P=13	P=12
1.000	S	S	S	$1.8 \cdot 10^{-4}$
1.001	0.088	0.070		
1.005		0.156	0.116	0.060
1.01	0.279	0.220	0.163	0.081
1.1	0.887	0.685	0.467	0.141
1.2	1.205	0.891	0.478	0.262
1.3	1.299	0.863	S	0.307
1.4	1.036	0.047	S	S
1.5	S	S		

**Table 6**

Truncation level (P)	Growth rate (r=0.3)	Growth rate (r=0.6)
2	$1.81 \cdot 10^{-1}$	$4.24 \cdot 10^{-1}$
4	$2.87 \cdot 10^{-2}$	$1.92 \cdot 10^{-1}$
6	$1.09 \cdot 10^{-2}$	$1.17 \cdot 10^{-1}$
8	$1.54 \cdot 10^{-3}$	$8.28 \cdot 10^{-2}$
10	$3.03 \cdot 10^{-4}$	$6.11 \cdot 10^{-2}$
12	$8.65 \cdot 10^{-5}$	$4.33 \cdot 10^{-2}$

